



Genetic abnormalities in a large cohort of Coffin–Siris syndrome patients

Futoshi Sekiguchi¹ · Yoshinori Tsurusaki^{1,2} · Nobuhiko Okamoto³ · Keng Wee Teik⁴ · Seiji Mizuno⁵ · Hiroshi Suzumura⁶ · Bertrand Isidor⁷ · Winnie Peitee Ong⁴ · Muzhirah Haniffa⁴ · Susan M. White^{8,9} · Mari Matsuo¹⁰ · Kayoko Saito¹⁰ · Shubha Phadke¹¹ · Tomoki Kosho¹² · Patrick Yap^{13,14} · Manisha Goyal¹⁵ · Lorne A. Clarke¹⁶ · Rani Sachdev¹⁷ · George McGillivray⁸ · Richard J. Leventer¹⁸ · Chirag Patel¹⁹ · Takanori Yamagata²⁰ · Hitoshi Osaka²⁰ · Yoshiya Hisaeda²¹ · Hirofumi Ohashi²² · Kenji Shimizu²² · Keisuke Nagasaki²³ · Junpei Hamada²⁴ · Sumito Dateki²⁵ · Takashi Sato²⁶ · Yasutsugu Chinen²⁷ · Tomonari Awaya^{28,29} · Takeo Kato²⁹ · Kougoro Iwanaga²⁹ · Masahiko Kawai²⁹ · Takashi Matsuoka³⁰ · Yoshikazu Shimoji³⁰ · Tiong Yang Tan^{8,9} · Seema Kapoor³¹ · Nerine Gregersen¹³ · Massimiliano Rossi³² · Mathieu Marie-Laure³² · Lesley McGregor³³ · Kimihiko Oishi³⁴ · Lakshmi Mehta³⁴ · Greta Gillies³⁵ · Paul J. Lockhart³⁵ · Kate Pope³⁵ · Anju Shukla³⁶ · Katta Mohan Girisha³⁶ · Ghada M. H. Abdel-Salam³⁷ · David Mowat³⁸ · David Coman³⁹ · Ok Hwa Kim⁴⁰ · Marie-Pierre Cordier⁴¹ · Kate Gibson⁴² · Jeff Milunsky⁴³ · Jan Liebelt⁴⁴ · Helen Cox⁴⁵ · Salima El Chehadeh⁴⁶ · Annick Toutain⁴⁷ · Ken Saida¹ · Hiromi Aoi^{1,48} · Gaku Minase¹ · Naomi Tsuchida¹ · Kazuhiro Iwama¹ · Yuri Uchiyama^{1,49,50} · Toshifumi Suzuki^{1,48} · Kohei Hamanaka¹ · Yoshiteru Azuma¹ · Atsushi Fujita¹ · Eri Imagawa^{1,34} · Eriko Koshimizu¹ · Atsushi Takata¹ · Satomi Mitsunashi¹ · Satoko Miyatake^{1,50} · Takeshi Mizuguchi¹ · Noriko Miyake¹ · Naomichi Matsumoto¹

Received: 15 July 2019 / Revised: 13 August 2019 / Accepted: 25 August 2019 / Published online: 17 September 2019
© The Author(s), under exclusive licence to The Japan Society of Human Genetics 2019

Abstract

Coffin–Siris syndrome (CSS, MIM#135900) is a congenital disorder characterized by coarse facial features, intellectual disability, and hypoplasia of the fifth digit and nails. Pathogenic variants for CSS have been found in genes encoding proteins in the BAF (BRG1-associated factor) chromatin-remodeling complex. To date, more than 150 CSS patients with pathogenic variants in nine BAF-related genes have been reported. We previously reported 71 patients of whom 39 had pathogenic variants. Since then, we have recruited an additional 182 CSS-suspected patients. We performed comprehensive genetic analysis on these 182 patients and on the previously unresolved 32 patients, targeting pathogenic single nucleotide variants, short insertions/deletions and copy number variations (CNVs). We confirmed 78 pathogenic variations in 78 patients. Pathogenic variations in *ARID1B*, *SMARCB1*, *SMARCA4*, *ARID1A*, *SOX11*, *SMARCE1*, and *PHF6* were identified in 48, 8, 7, 6, 4, 1, and 1 patients, respectively. In addition, we found three CNVs including *SMARCA2*. Of particular note, we found a partial deletion of *SMARCB1* in one CSS patient and we thoroughly investigated the resulting abnormal transcripts.

Introduction

Coffin–Siris syndrome (CSS, MIM#135900) is an autosomal dominant developmental disorder exhibiting, coarse

facial features, hypoplasia of the fifth digit/nails, hypotonia, hypertrichosis, and sparse scalp hair [1]. In 2012, pathogenic CSS variants were reported in genes encoding subunits of the BAF (BRG1-associated factor) chromatin-remodeling complex [2, 3]. Since then, more than 150 CSS individuals have been molecularly diagnosed [4–10]. Nine genes have so far been found to be involved in the pathogenesis of CSS: *ARID1A* (MIM# 614607), *ARID1B* (MIM# 135900), *ARID2* (MIM# 617808), *SMARCA4* (MIM# 614609), *SMARCB1* (MIM# 614608), *SMARCE1* (MIM# 616938), *SOX11* (MIM# 600898), *PHF6* (MIM# 300414),

Supplementary information The online version of this article (<https://doi.org/10.1038/s10038-019-0667-4>) contains supplementary material, which is available to authorized users.

✉ Naomichi Matsumoto
naomat@yokohama-cu.ac.jp

Extended author information available on the last page of the article

and *DPF2* (MIM# 618027). These genes encode components of the BAF complex, except for *SOX11* and *PHF6*. *SOX11* encodes a transcriptional factor that binds to SMARCA4 and plays a role in embryonic neurogenesis [5, 11], and *PHF6* regulates transcription by interacting with another ATP-dependent chromatin remodeler, the nucleosome remodeling and deacetylation complex [4, 12].

The BAF complex is a mammalian SWI/SNF (SWItch/Sucrose Non-Fermentable) complex that plays an important role in chromatin remodeling [13]. The BAF complex is required for normal mammalian organ development, and mutations in genes encoding BAF complex subunits cause multiple malformations and developmental disorders, including CSS [14–16].

Presently, more than 150 CSS individuals with a pathogenic variant are described in the literature [17]. We previously reported 71 CSS individuals of whom 39 pathogenic variants were found [2, 18]. Since then, we have recruited 182 additional CSS-suspected individuals. We have analyzed these patients together with the 32 individuals for whom no molecular diagnosis was achieved and we present the results of a comprehensive genetic analysis.

Materials and methods

Recruitment of subjects

We newly recruited 182 individuals clinically suspected of CSS and analyzed them together with 32 CSS individuals for whom no molecular diagnosis had been determined [2, 18]. The diagnostic criteria have not yet been completely established, but most patients shared several key phenotypes including developmental delay, hypoplastic digits/nails, body hypertrichosis, and coarse face according to the clinicians who saw patients [19, 20]. Differential diagnoses should include Nicolaides–Baraitser syndrome (NCBRS), deafness, onychodystrophy, osteodystrophy, mental retardation, and seizures syndrome, and so on, but it was sometimes difficult for them to completely differentiate them from CSS [4, 21, 22]. This study was approved by the institutional review board of the Yokohama City University Faculty of Medicine.

DNA preparation

Peripheral blood leukocytes or saliva of individuals and their family members were collected after obtaining informed consent and genomic DNA was extracted by standard methods.

Whole exome sequencing

Whole exome sequencing (WES) was performed as previously reported [23]. Coding regions within the genomic DNA were enriched with the SureSelect Human All Exon V4, V5, or V6 kit (Agilent Technologies) and sequenced on a HiSeq 2000 or 2500 platform (Illumina, San Diego, CA) [24]. After sequencing, raw FASTQ files were processed to Variant Call Format (VCF) files through several steps, with the following tools: Novoalign, SAMtools, Picard, and Genome Analysis Tool kit. VCF files were annotated by ANNOVAR. All variants [including single nucleotide variants (SNVs) and short insertions/deletions (indels)] were filtered by allele frequency using a public database, The Exome Aggregation Consortium (ExAC), Exome Sequencing Project v.6500 (ESP6500), the Human Genetic Variation Database, and our in-house database ($n = 575$). In parallel, BAM files were used for copy number variation (CNV) analysis using the Nord method [25], and eXome-Hidden Markov Model [26], as previously reported [27, 28]. Candidate SNVs were validated by Sanger sequencing using an ABI capillary sequencer, 3130xL or 3500xL (Thermo Fisher Scientific). Candidate CNVs were validated by quantitative polymerase chain reaction (qPCR) using a Rotor-Gene Q with Rotor-Gene 6000 Series Software 1.7 (Qiagen) or a LightCycler 480 with LightCycler 480 Software, Version 1.5 (Roche).

Mutation load score (MLS)

To evaluate the mutation load of a single exon as a function of its size, we collected missense variants in each genes which are registered in gnomAD (as of June 2019). Next we calculated the accumulation of missense variants within each exon, except for *SOX11* which consists of only one exon, and adjusted by length of each exon and multiplied by 100, as Bögershausen et al. advocated it as mutation load score (MLS) [29]. MLS in this study means the number of missense variants per 100 bp in each exon.

Reverse transcription PCR (RT-PCR)

cDNA was examined to validate effects of a truncating variant and a deletion in patients CSS235 and CSS076, respectively. Total RNA was extracted from their lymphoblastoid cells with an RNeasy Plus Mini Kit (QIAGEN). Subsequently, cDNA was synthesized with the SuperScript III First-Strand Synthesis System (Thermo Fisher Scientific) using oligo dT primers, or with the PrimeScript first strand cDNA Synthesis Kit (Takara Bio) using random hexamer primers, according to the manufacturers' instructions. PCR and Sanger sequencing were performed using specific primers for each abnormality using the 3130xl or 3500xl

capillary sequencer. Primer information is available on request.

Results

Overview of pathogenic gene variants

A total of 214 individuals with suspected CSS (182 newly recruited and 32 for whom no molecular diagnosis was determined in a previous study [2, 18]) were analyzed by WES. Among these, 57 individuals were excluded from the study because they had pathogenic variants in genes that cause different diseases such as NCBRS (seven individuals), Wiedemann–Steiner syndrome (five individuals), and KBG syndrome (two individuals) (Fig. 1a). In the remaining 157 individuals, 78 had pathogenic variants (49.6%) (71 SNVs and 7 CNVs). (Fig. 1a, b). All variants found in this study are shown in Table 1. Four SNVs (three variants in *SOX11* and one variant in *SMARCE1*) and two CNVs (two duplications involving the entire *SMARCA2* locus) have been previously described by our group [5, 11, 30, 31], but are included here to give an overview of the pathogenic variants in this CSS cohort. Among 71 pathogenic SNVs, 55 occurred de novo, 15 could not be confirmed as de novo because parental samples were unavailable, and only one in *PHF6* (X-linked) was inherited from his healthy mother. Among seven pathogenic CNVs, three occurred de novo, two could not be confirmed because of a lack of parental samples, and two were balanced chromosomal translocations inherited from their healthy mothers (Table 1).

ARID1B

Forty-eight *ARID1B* variants were found in our CSS cohort (45 SNVs and 3 CNVs), accounting for 61.5% of genetically resolved cases (48/78) (Table 1 and Fig. 1b). Twenty-eight were novel. Various types of variants included stop-gain, frameshift insertion/deletion, splice site changes and CNVs, clearly indicating that loss-of-function (LoF) changes in *ARID1B* cause CSS. Of note, one missense variant, c.6257T>G:p.(Leu2286Arg) was found in the BAF250c domain. Only two pathogenic missense variants in *ARID1B* were registered in HGMD: c.5998G>T: p.Asp2000Tyr in an individual with short stature (not associated with CSS) [32], and c.6092T>C:p.Ile2031Thr in an individual with corpus callosum abnormalities (also not associated with CSS) [33].

Causative variants appear to be preferentially located in exons 1 and 20, but after exon-size correction no such exonic accumulation was seen (Fig. 2a). We are aware that missense variants and LoF variants in healthy populations are registered in gnomAD. Only 10 variants that passed

quality control were registered as LoF: five frameshift variants and five variants located in canonical splice sites. Frameshift variants are found in exon 1 ($n = 1$) and exon 20 (last exon, $n = 4$). Canonical splice variants were also found in the middle of *ARID1B*: splice acceptor sites of exon 5, 8, and 11, in the splice donor site of exon 12, and deep in intron 11 (c.3135 + 729insG), but importantly the variant deep in intron 11 could be a canonical splice variant for another transcript (NM_001346813.1:c.3097-2insG). In gnomAD, additional missense variants in healthy populations were clustered in exons 2, 11, and 12 (Fig. 2a) but, in the current study, CSS-causative missense variant, c.6257T > G:p.(Leu2286Arg), occurred in exon 20.

ARID1A

Six *ARID1A* variants were found in six individuals: two frameshift, two canonical splice-site, one stop-gain and one missense, indicating that *ARID1A* variants are LoF (Table 1 and Figs. 1b, 2b). All were novel. Interestingly, c.6251T>G: p.(Val2084Gly) is located within the BAF250c domain, similar to the *ARID1B* missense variant. In the HGMD database, only one pathogenic *ARID1A* missense variant, c.6232G>A: p.(Glu2078Lys), was registered as causing CSS and is located within the BAF250 domain [34]. Pathogenic variants in *ARID1A* were distributed throughout the gene (Fig. 2b) and were not accumulated in any exons after exon-size standardization (data not shown). In contrast, missense variants in gnomAD were accumulated in exons 5, 16, and 19. Only four LoF variants were registered: two frameshift variants in the first exon and two canonical splicing variants, similar to *ARID1B*.

SMARCA4

Six missense variants in *SMARCA4* were found in seven CSS individuals (one recurrent variant found in two independent cases) (Table 1 and Figs. 1b, 3a). All six variants occurred de novo and four were novel. All variants were located within functional domains. Interestingly, pathogenic variants were located in variant-poor exons in gnomAD (Fig. 3a).

SMARCB1

Seven pathogenic SNVs and one CNV were found in eight CSS patients in this cohort (Table 1 and Fig. 3b). Six variants were novel. Seven out of eight pathogenic variants occurred de novo, one variant found in patient CSS174 could not be confirmed because parental samples were unavailable. The most common pathogenic variant, c.1091_1093delAGA, was found in two patients of this cohort and has been found in other cohorts [2, 9]. In patient

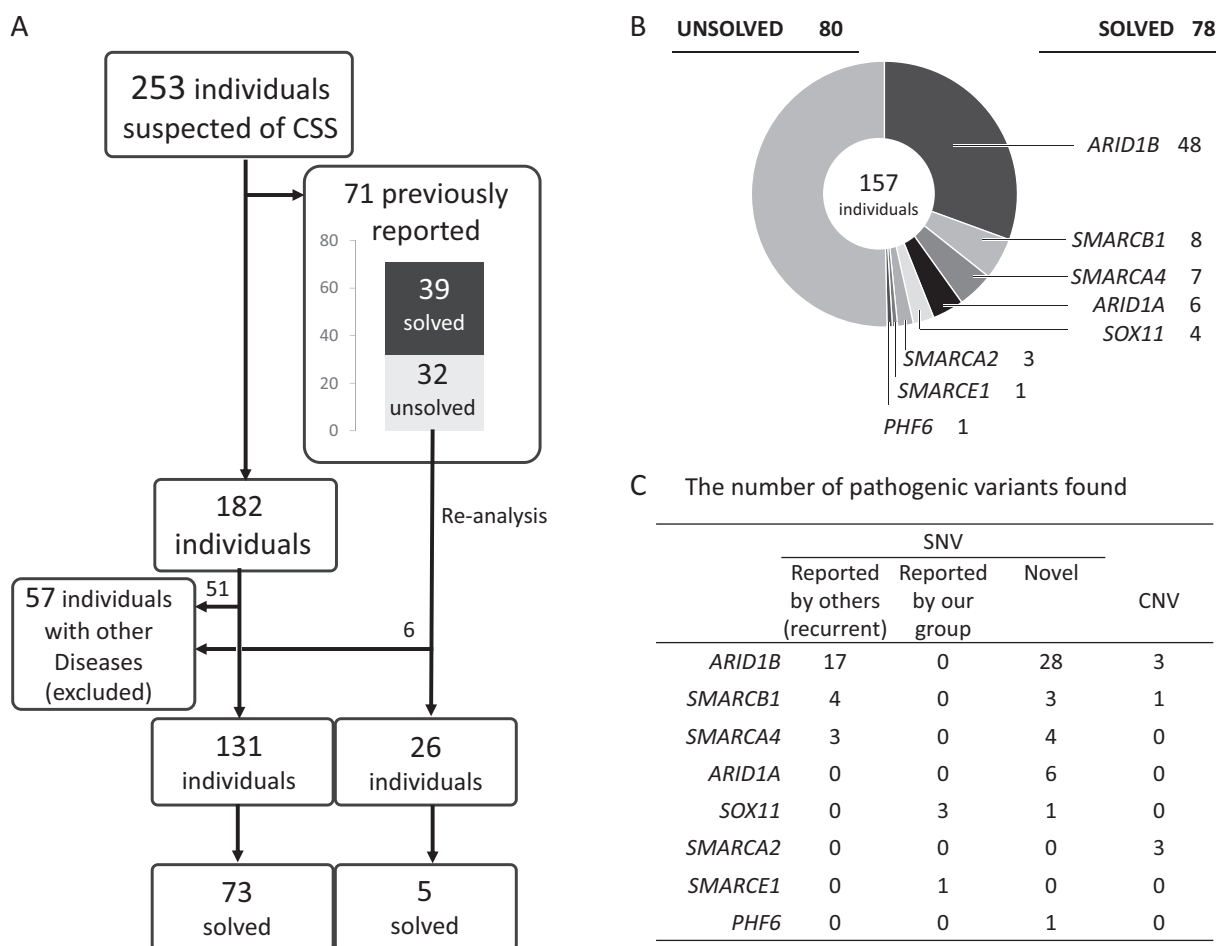


Fig. 1 Flow chart of the analysis in this study. **a** In addition to 71 previously reported CSS patients [18], we recruited another 182 CSS patients. All the new patients were analyzed by WES and the 32 undefined patients from the previous study were subjected to re-analysis of existing WES data. Among 214 patients, 57 had pathogenic variants for other diseases and were therefore excluded from the study. **b** Pie chart of mutated genes in 157 individuals in this study. **c** Number of pathogenic variants in each gene. Pathogenic variants

already registered in HGMD were counted as ‘SNV_reported by others (recurrent)’ or ‘SNV_reported by our group’ and those which were not registered were categorized as ‘SNV_novel’. Pathogenic CNVs were simply counted as their size and position as they are basically private. Two SNVs in *SOX11* were reported by Tsurusaki et al. [5], one SNV in *SOX11* was reported by Okamoto et al. [11], one SNV in *SMARCE1* was reported by Zarate et al. [31], and two CNVs involving *SMARCA2* were reported by Miyake et al. [30]

CSS235, the frameshift insertion, c.1052dup, might not be subjected to nonsense-mediated mRNA decay as it was 66 bp from the 3'-end of exon 8, the second last exon. RT-PCR using lymphoblastoid cells derived from the patient showed consistent aberrant mRNA expression regardless of cycloheximide treatment (Supplementary Fig. 1). Furthermore, individual CSS076 had a 9001-bp deletion from intron 8 through the end of the gene extending to the neighboring *DERL3* gene (Fig. 4). RT-PCR using lymphoblastoid cells derived from CSS076 showed two aberrant transcripts regardless of cycloheximide treatment. One transcript involved exon 8, intron 8 and genomic sequences after a telomeric deletion breakpoint. Another shorter transcript contained exon 8 and 112 bp of genomic sequence after the telomeric deletion breakpoint. Unfortunately, we could not

determine full-length cDNA sequences because of many repeated sequences, including SINEs and poly A repeats in the vicinity of the 3'-end of both transcripts. However, we could confirm the stop codon in two transcripts and consequently could predict amino acid sequences, p.Arg374-Tyrfs*48 and p.Arg374Aspfs*110. Both predicted proteins have longer amino acid sequences (with an almost preserved SNF5 domain) than the wild-type protein. Interestingly two aberrant shorter transcripts may lead to longer aberrant protein products than the wild-type protein produced by the wild-type transcript. In addition, a predicted 48 amino acid sequence produced by a longer aberrant transcript does not have any functional domains, but a predicted 110 amino acid sequence produced by a shorter aberrant transcript had a presumed SERPIN domain

Table 1 The pathogenic variants and variations found in this study

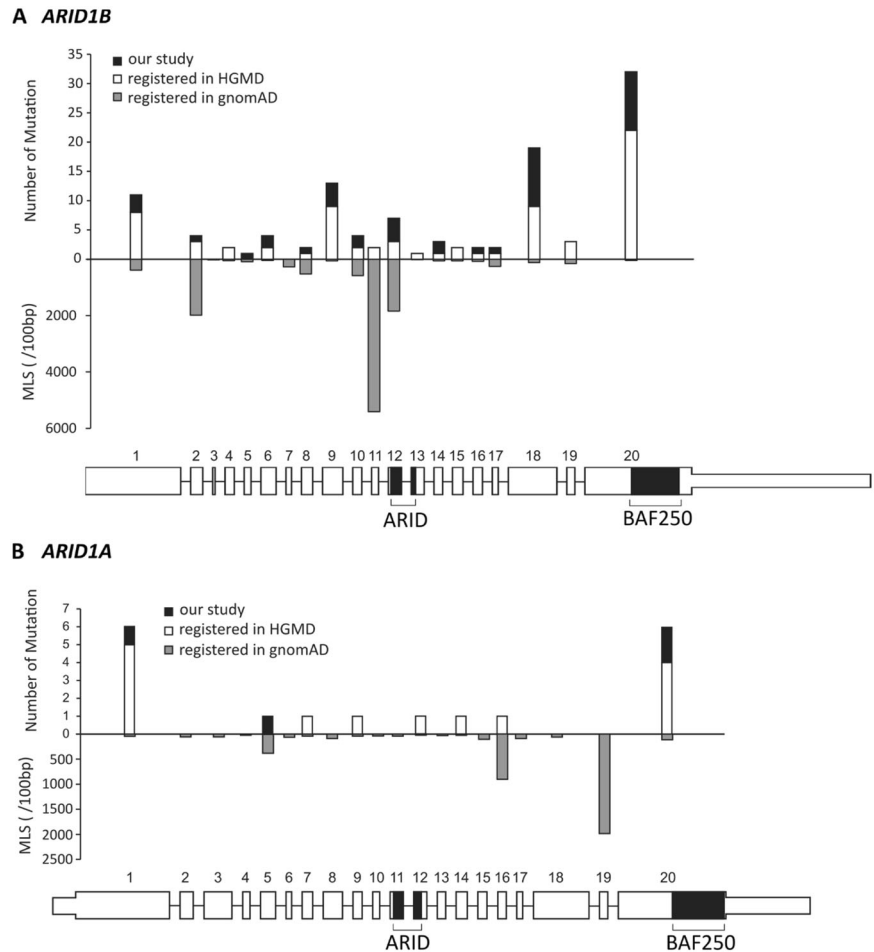
Gene	RefSeq accession No	Project ID	Nucleotide change	Amino acid change	Inheritance	Novel or reported	Reference
SNV							
<i>ARID1B</i>	NM_020732.3	33	c.1151dup	p.Gly385Argfs*150	n/a	novel	
		78	c.2552-2A>C		de novo	novel	
		80	c.1983del	p.Lys661Asnfs*7	de novo	novel	
		81	c.6083del	p.Leu2028Trpfs*8	n/a	novel	
		85	c.4063_4064del	p.Gln1355Alafs*103	de novo	novel	
		89	c.3262dup	p.Ser1088Phefs*30	de novo	novel	
		90	c.3345+1G>A		n/a	novel	
		91	c.4422dup	p.Tyr1475Leufs*35	de novo	novel	
		92	c.4870C>T	p.Arg1624*	de novo	reported	Al-Shamsi et al. [27]
		94	c.3292_3293insA	p.Leu1098Hisfs*20	n/a	novel	
		97	c.2195dup	p.Ser736Ilefs*27	de novo	novel	
		102	c.2952dup	p.Asn985Glnfs*4	de novo	novel	
		108	c.1727del	p.Pro576Leufs*17	n/a	novel	
		110	c.4552C>T	p.Gln1518*	de novo	novel	
		117	c.5394_5397del	p.Phe1798Leufs*52	de novo	reported	Santen et al. [35]
		122	c.2881C>T	p.Gln961*	de novo	novel	
		127	c.3898C>T	p.Gln1300*	n/a	novel	
		128	c.4736dup	p.Met1580Aspfs*56	de novo	novel	
		132	c.2482del	p.Ile828Serfs*17	de novo	novel	
		135	c.4183_4184insG	p.Gln1395Argfs*64	n/a	novel	
		148	c.4870C>T	p.Arg1624*	de novo	reported	Al-Shamsi et al. [27]
		151	c.3586C>T	p.Gln1196*	de novo	novel	
		161	c.3304C>T	p.Arg1102*	n/a	reported	
		164	c.5394_5397del	p.Phe1798Leufs*52	n/a	reported	Santen et al. [35]
		168	c.3586dup	p.Gln1196Profs*14	de novo	reported	Wieczorek et al. [4]
		169	c.2692C>T	p.Arg898*	de novo	reported	Wieczorek et al. [4]
		181	c.6553_6554dup	p.Pro2186Argfs*8	de novo	novel	
		183	c.6190C>T	p.Gln2064*	de novo	novel	
		185	c.5404C>T	p.Arg1802*	de novo	reported	Fitzgerald et al. [9]
		188	c.4870C>T	p.Arg1624*	de novo	reported	Al-Shamsi et al. [27]
		194	c.2692C>T	p.Arg898*	de novo	reported	Wieczorek et al. [4]
		199	c.1222del	p.Gln408Argfs*22	de novo	novel	
		200	c.5173del	p.Ala1725Glnfs*41	de novo	novel	
		202	c.6604_6608del	p.Leu2202Serfs*38	de novo	novel	
		203	c.3304C>T	p.Arg1102*	de novo	reported	Wieczorek et al. [4]
		216	c.6257T>G	p.Leu2086Arg	de novo	novel	
223	c.5776C>T	p.Arg1926*	de novo	reported	Mignot et al. [33]		
233	c.4390_4391del	p.Met1464Valfs*6	n/a	novel			
234	c.1392_1402del	p.Gln467Argfs*64	de novo	reported	Tsurusaki et al. [5]		
236	c.4846dup	p.Ser1616Phefs*20	n/a	novel			
247	c.2692C>T	p.Arg898*	n/a	reported	Wieczorek et al. [4]		
249	c.2248C>T	p.Arg750*	de novo	reported	Wieczorek et al. [4]		
252	c.2641C>T	p.Gln881*	de novo	novel			
255	c.4336C>T	p.Gln1446*	n/a	novel			
260	c.5025+1G>C		de novo	reported	Chérot et al. [10]		

Table 1 (continued)

Gene	RefSeq accession No	Project ID	Nucleotide change	Amino acid change	Inheritance	Novel or reported	Reference
<i>ARID1A</i>	NM_006015.4	54	c.3199-15G>A		n/a	novel	
		79	c.5708del	p.Pro1903Glnfs*20	de novo	novel	
		146	c.6251T>G	p.Val2084Gly	de novo	novel	
		176	c.802C>T	p.Gln268*	de novo	novel	
		190	c.4102-1G>A		de novo	novel	
		192	c.2159del	p.Pro720Glnfs*22	de novo	novel	
<i>SMARCA4</i>	NM_001128849.1	96	c.1345G>A	p.Glu449Lys	de novo	novel	
		100	c.3526A>G	p.Ser1176Gly	de novo	novel	
		105	c.3557C>T	p.Ala1186Val	de novo	novel	
		113	c.3376C>T	p.Leu1126Phe	de novo	novel	recurrent with CSS116
		116	c.3376C>T	p.Leu1126Phe	de novo	novel	recurrent with CSS113
		162	c.1561C>T	p.Arg521Trp	de novo	novel	
		173	c.2576C>T	p.Thr859Met	de novo	reported	Tsurusaki et al. [2]
<i>SMARCB1</i>	NM_003073.3	88	c.1096C>G	p.Arg366Gly	de novo	reported	Wieczorek et al. [4]
		136	c.1091_1093del	p.Lys364del	de novo	reported	Tsurusaki et al. [2]
		156	c.806A>G	p.His269Arg	de novo	novel	
		174	c.1091_1093del	p.Lys364del	n/a	reported	Tsurusaki et al. [2]
		180	c.1087A>G	p.Lys363Glu	de novo	novel	
		230	c.1121G>A	p.Arg374Gln	de novo	reported	Wieczorek et al. [4]
		235	c.1052dup	p.Leu352Thrfs*9	de novo	novel	
<i>SMARCE1</i>	NM_003079.4	114	c.314G>A	p.Arg105Gln	de novo	reported	Zarate et al. [31]
<i>SOX11</i>	NM_003108.3	26	c.347A>G	p.Tyr116Cys	de novo	reported	Tsurusaki et al. [5]
		43	c.178T>C	p.Ser60Pro	de novo	reported	Tsurusaki et al. [5]
		177	c.305C>T	p.Ala102Val	de novo	reported	Okamoto et al. [11]
		212	c.154C>T; c.235A>G	p.Pro52Ser; p.Ile79Val	de novo	novel	
<i>PHF6</i>	NM_032458.2	239	c.802G>A	p.Val268Ile	hemi, inherited from mother	novel	
CNV							
<i>ARID1B</i>		39	partial deletion		n/a		
		72	entire gene deletion		de novo		
		83	partial deletion		n/a		
<i>SMARCB1</i>		76	partial deletion		de novo		
<i>SMARCA2</i>		125	duplication	dup(9)(p24.3p22.2)	de novo	reported	Miyake et al. [30]
		131	duplication	46,XX, der(6)t(6;9)(p25;p21)	inherited from mother with balanced translocation (46,XX, t(6;9)(p25;p21))	reported	Miyake et al. [30]
		154	duplication	der(4)t(4;9)(q35.1:p21.3)	inherited from mother with balanced translocation (t(4;9)(q35.1:p21.3))		

SNV single nucleotide variant, CNV copy number variant, n/a not available

Fig. 2 Graphical presentation of pathogenic variants corresponding to exons in *ARID1B* and *ARID1A*. Pathogenic variant count is shown as a bar above each exon. White bars show the number of pathogenic variants registered in the HGMD database, and black bars show the number of pathogenic variants found in this study. While exon size (box) reflects original physical length, introns (line) are shown as the same length. Functional domains are shown as black boxes. The mutation load scores (MLS: number of mutations per 100 bp) of variants registered in gnomAD are shown by gray bars. **a** Variants of *ARID1B* (NM_020762.3). Pathogenic variants are seen in all exons. Longer exons harbor more pathogenic variants. **b** Variants of *ARID1A* (NM_006015.4). Longer exons contain more pathogenic variants



(Supplementary Fig. 2). Interestingly, the amino acid sequence of the SNF5 domain in p.Arg374Tyrfs*48, p.Arg374Aspfs*110 and the wild-type protein is the same except for the last amino acid. The deletion involving intron 8 and beyond led to aberrant proteins associated with CSS. Thus, this may not be a loF variant, rather a gain-of-function variant.

SMARCE1

Only one previously reported missense variant (by our group) was found [31] (Table 1 and Fig. 3c). This variant was located in the high mobility group box domain (HMG domain, IPR009071) [31]. Missense variants in healthy populations of gnomAD were clustered in exons 10 and 11 where no functional domain was recognized.

ARID2 and DPF2

We found no variants of these genes in our cohort.

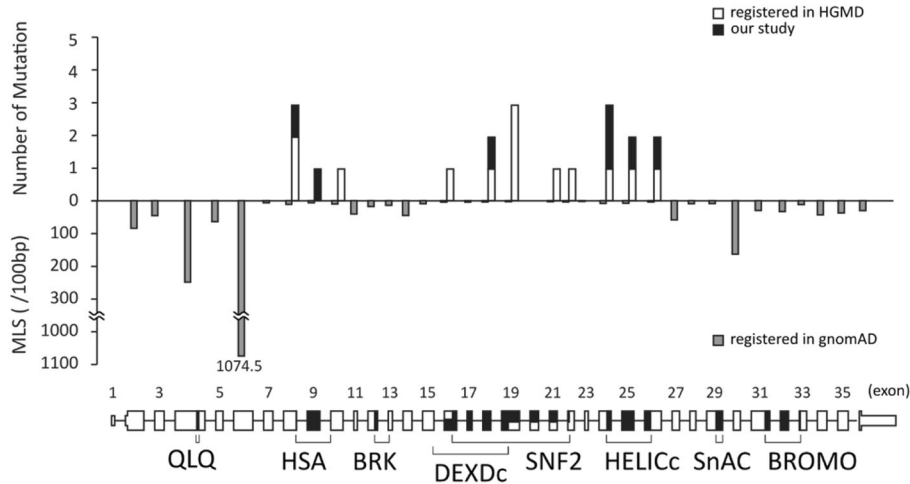
SOX11 and PHF6

We found four pathogenic variants (including one novel) in *SOX11* in four patients, and one novel pathogenic *PHF6* variant in one patient (Table 1 and Fig. 3d, e). One *SOX11* variants and one *PHF6* variant were novel. All *SOX11* pathogenic variants found in this and other studies were missense variants within the high mobility group box domain (HMG domain, IPR009071) [5, 11]. The pathogenic missense variant found in *PHF6* was located in the extended PHD domain (ePHD domain, IPR034732).

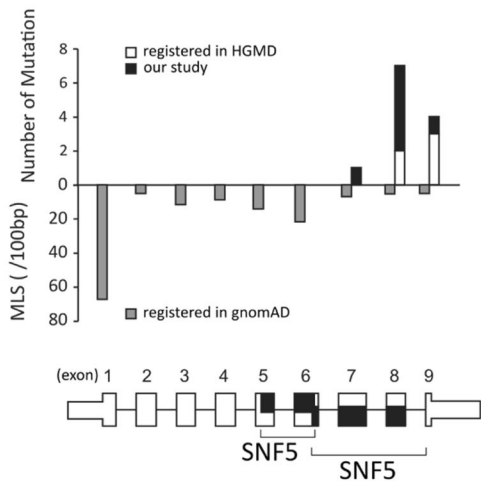
The other genes

Three CNVs involving *SMARCA2* were found in our cohort. Two of them were reported previously [30]. A new case (CSS154) with *SMARCA2* duplication is derived from balanced translocations in the mother. Her karyotype is presumed to be der(4)t(4;9)(q35.1;p21.3) (Table 1).

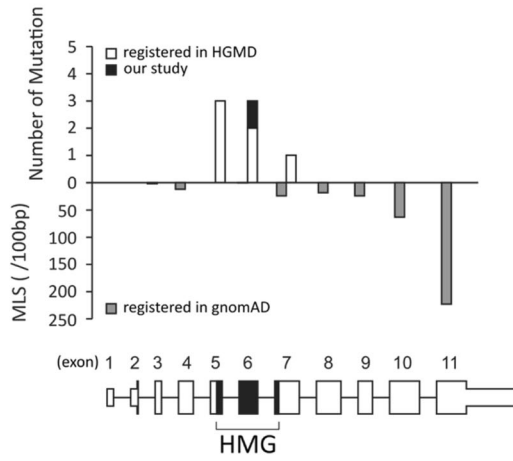
A SMARCA4



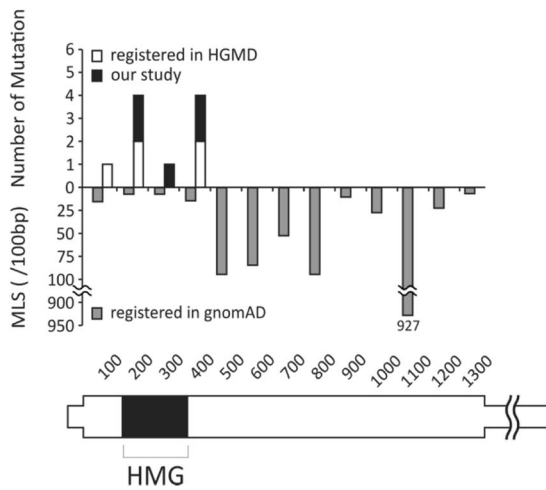
B SMARCB1



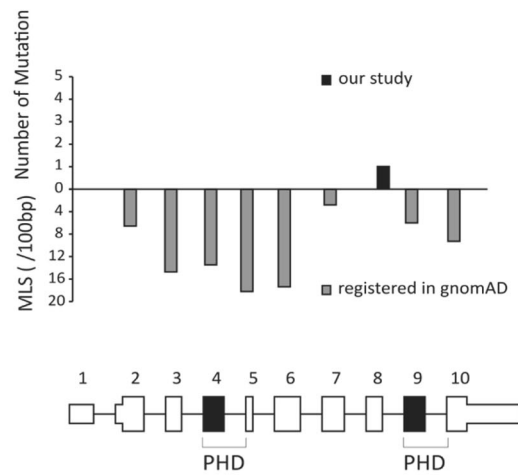
C SMARCE1



D SOX11 (single exon)



E PHF6



◀ **Fig. 3** Graphical presentation of pathogenic variant count corresponding to exons of *SMARCA4*, *SMARCB1*, *SMARCE1*, *SOX11*, and *PHF6*. Pathogenic variant count is shown by a bar above each exon. White bars show the number of pathogenic variants registered in the HGMD database, and black bars show the number of pathogenic variants found in this study. While exon size (box) reflects original physical length, introns (line) are shown as the same length. Functional domains are shown as black boxes. The mutation load scores (MLS: number of mutations per 100 bp) of variants registered in gnomAD are shown by gray bars. **a** Variants of *SMARCA4* (NM_001128849.1), **b** *SMARCB1* (NM_003073.4), **c** *SMARCE1* (NM_003079.4), **d** *SOX11* (NM_003108.3), and **e** *PHF6* (NM_032458.2). *SOX11*, a single exon gene, is displayed with every 100 bp indicated

Discussion

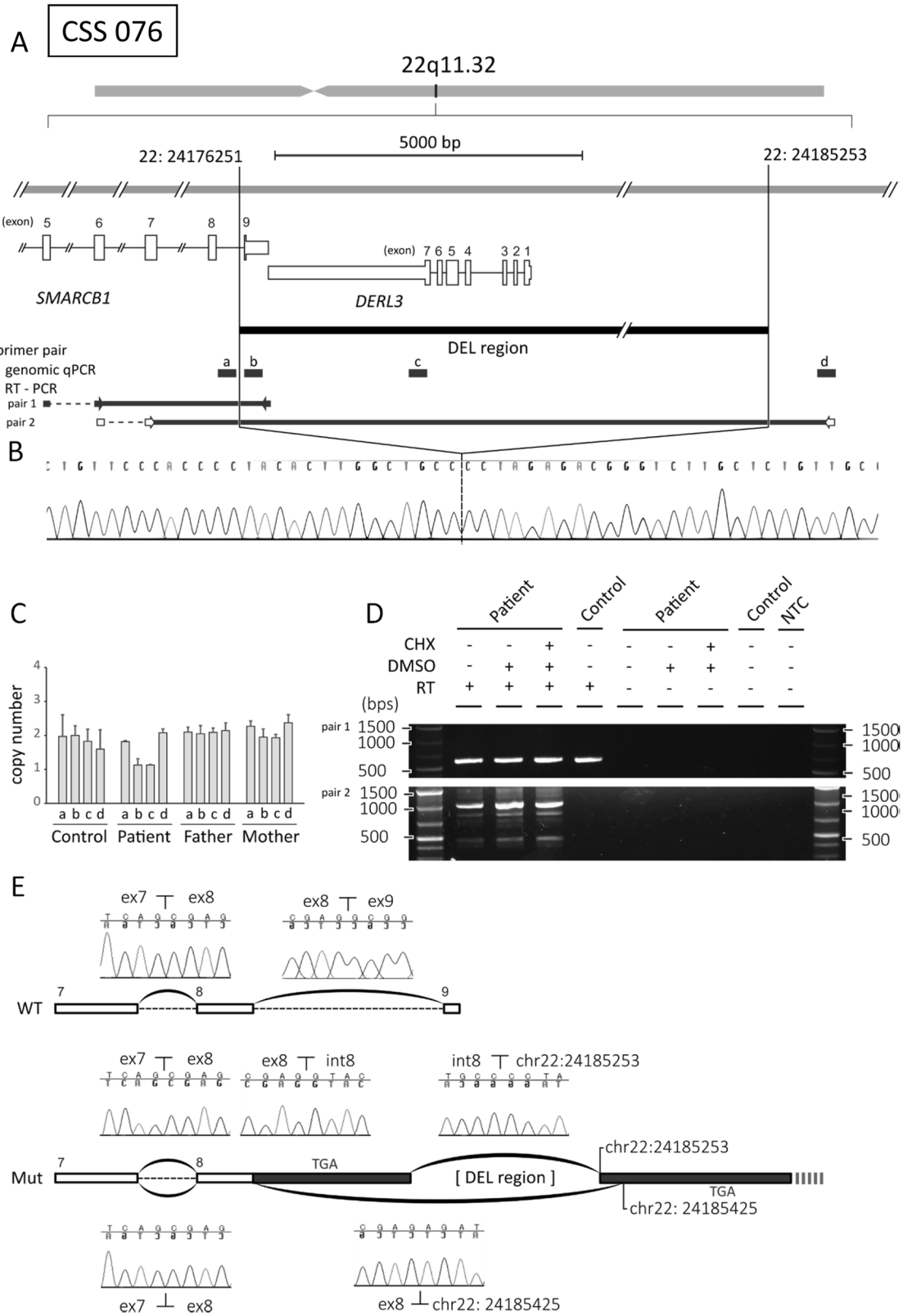
Genetic variants in CSS were detected by next generation sequencing. To date, nine genes have been registered as CSS disease genes, and over 150 patients with pathogenic variants were reportedly diagnosed with CSS. In 182 newly recruited and 32 undefined patients from our previous cohort, 57 patients with pathogenic variants in various genes that cause other diseases were excluded from further analysis (Fig. 1a). In the remaining 131 newly recruited patients, 73 had pathogenic variants in CSS genes (55.7%). This detection rate is similar to that of previous studies (54.9–71 %) [4, 18, 35]. In the 32 previously undefined patients [18], we identified three pathogenic variants in *ARID1B* (one SNV in CSS033, and two CNVs in CSS039 and CSS072, see Table 1), two in *SOX11* in CSS026 and CSS043, which have already been described elsewhere [5], and six in genes causing other diseases. In total we detected 78 patients (73 newly recruited and five previously undefined) with pathogenic variations. Forty-eight *ARID1B*, six *ARID1A*, seven *SMARCA4*, eight *SMARCB1*, three *SMARCA2*, one *SMARCE1*, four *SOX11*, and one *PHF6* variants were found. No pathogenic variant was identified in *ARID2* or *DPF2*. As expected, the most common variants in this cohort were in *ARID1B*. Of note, several pathogenic missense variants in *PHF6* have been reported in Börjeson–Forssman–Lehmann syndrome (BFLS: OMIM 301900) [36–38]. Patients with a pathogenic *PHF6* variant who were initially diagnosed as CSS in early childhood [4] were later diagnosed as BFLS [6]. As our patient was diagnosed before the age of 1 year, it remains to be seen how his phenotype will evolve and whether his diagnosis will remain CCS or be changed to BFLS later.

In contrast to various types of variants found in *ARID1B* and *ARID1A* such as missense, nonsense, splicing substitutions, small insertion/deletion variants and gross changes, *SMARCA4*, *SMARCB1*, and *SMARCE1* variants maintain the overall protein sequence (almost all were missense variants or an in frame 3-bp deletion). As most

missense variants in these genes are positioned within functional domains, they are expected to alter the wild-type protein function. For example, all missense variants in *SMARCB1* were located within the SNF domain, which is a highly conserved and core component of this protein [39]. Interestingly, nonsense, truncating, or frameshift variants in *SMARCB1* have only been found in preliminary stage tumors, including in malignancy or tumor predisposition syndrome [40], but never in CSS. Of note, we identified one frameshift variant, c.1052dup, p.Leu352Thrfs*9 and a deletion involving intron 8 and exon 9 (the last exon) of *SMARCB1* and its downstream gene (der1-like domain family, member 3 (*DERL3*)) in two CSS patients (CSS235 and CSS076, respectively). Interestingly, both changes did not lead to nonsense-mediated mRNA decay because of newly created stop codons in the downstream sequence. Therefore these two exceptional changes in *SMARCB1* may lead to altered protein function. The genomic deletion in CSS076 also involved *DERL3*, which encodes a Derlin family protein that localizes to the endoplasmic reticulum (ER) and plays a role in the degradation of misfolded glycoproteins in the ER [41]. Many LoF *DERL3* variants are registered in gnomAD with pLI scores = 0.00; therefore, *DERL3* is unlikely to be a haploinsufficient gene. Thus, we concluded that *DERL3* deletion did not contribute to the CSS phenotype.

Pathogenic *SMARCB1* variants in CSS were clustered in the last two exons (exon 8 and 9), while those in schwannoma occur mostly in the first three and last three exons. In contrast, truncating variants throughout the entire gene and gross deletions in *SMARCB1* are associated with malignancy, as in rhabdoid tumor [40]. *SMARCB1* deletion, even a partial deletion, has never been described in CSS [40]. In this study, we highlighted two novel *SMARCB1* variants, both of which affect the SNF5 domain. Despite many studies of *SMARCB1* deletions that result in incomplete recruitment of SWI/SNF subunits [39, 42, 43], no functional studies specifically targeting the SNF5 domain or C terminus of *SMARCB1* have been reported. Together with the other pathogenic variants found in CSS that are confined to exons 8 and 9, these two novel variants highlight the importance of the SNF5 domain and C terminus in the pathogenicity of CSS.

In conclusion, we report a comprehensive genetic analysis of the largest CSS cohort ever assembled. We found pathogenic variants in 55.7% of newly recruited individuals and three CNVs in initially ‘unsolved’ individuals. Most of the pathogenic variants identified replicated previous findings of other cohorts, although many novel variants and two unique variants in *SMARCB1* were also detected. However, over 40% of individuals with CSS remain genetically uncharacterized. Several studies of other Mendelian diseases achieved diagnostic success by using a combination



◀ **Fig. 4** Analysis of *SMARCB1* cDNA in CSS076 with a 9-kb deletion involving *SMARCB1*. **a** A physical map around a 9.0-kb deletion involving *SMARCB1* and *DERL3* in CSS076. Positions of primer pairs for quantitative PCR are shown as rectangles a–d, which correspond to a–d in c. **b** Sequence of breakpoint PCR product. The deletion was 9001 bp in size. **c** Quantitative PCR using primer pairs b and c confirmed the heterozygous deletion. **d** RT-PCR analysis of *SMARCB1* cDNA. Upper and lower panels show product amplified with primer pair 1 and 2, respectively. RT-PCR with primer pair 1 amplified cDNA of the patient and a control. RT-PCR with primer pair 2 amplified only the patient's cDNA. RT-PCR with primer pair 2 showed two cDNA products of ~500 and 1000 bp. Arrowhead indicates an ~500-bp band. **e** *SMARCB1* cDNA structure (NM_003073.4). White boxes show protein coding exons, while dark gray boxes show new exonic regions created by the deletion that are not present in the wild-type protein. Dotted lines show *SMARCB1* introns. Arched lines above and below break lines between boxes show connections of cDNA sequences. RT-PCR using primer pair 1 amplified only a wild-type fragment. RT-PCR with primer pair 2 produced longer and shorter products. The longer product had wild-type sequence from the end of exon 8, through intron 8 until the centromeric deletion breakpoint and sequence after the telomeric deletion breakpoint. The shorter product skipped intron 8 and extended beyond the telomeric deletion breakpoint. The longer product had a stop codon in intron 8, and the shorter product had a stop codon after the telomeric deletion breakpoint

of approaches, such as RNA sequencing [44] or whole genome sequencing [45, 46]. Our study can, therefore, be improved by further extensive analyses using other methods.

Acknowledgements We thank the patients and their family for participating in this work. We also thank Ms N. Watanabe, Ms K. Takabe and Ms S. Sugimoto for their excellent technical assistance. This work was supported by AMED under the grant numbers JP19ek0109280, JP19dm0107090, JP19ek0109301, JP19ek0109348, and JP18kk020501 (to NM); JSPS KAKENHI under the grant numbers JP17H01539 (to NM) and JP19H03621 (to NM); grants from the Ministry of Health, Labor, and Welfare (to NM); and the Takeda Science Foundation (to NM and NM). We thank Jeremy Allen, PhD, from Edanz Group (www.edanzediting.com/ac) for editing a draft of this manuscript.

Compliance with ethical standards

Conflict of interest The authors declare that they have no conflict of interest.

Publisher's note Springer Nature remains neutral with regard to jurisdictional claims in published maps and institutional affiliations.

References

- Coffin GS, Siris E. Mental retardation with absent fifth fingernail and terminal phalanx. *Am J Dis Child*. 1960;1970:433–9.
- Tsurusaki Y, Okamoto N, Ohashi H, Kosho T, Imai Y, Hibi-Ko Y, et al. Mutations affecting components of the SWI/SNF complex cause Coffin-Siris syndrome. *Nat Genet*. 2012;44:376–8.
- Santen GW, Aten E, Sun Y, Almomani R, Gilissen C, Nielsen M, et al. Mutations in SWI/SNF chromatin remodeling complex gene ARID1B cause Coffin-Siris syndrome. *Nat Genet*. 2012;44:379–80.
- Wieczorek D, Bogershausen N, Beleggia F, Steiner-Haldenstatt S, Pohl E, Li Y, et al. A comprehensive molecular study on Coffin-Siris and Nicolaides-Baraitser syndromes identifies a broad molecular and clinical spectrum converging on altered chromatin remodeling. *Hum Mol Genet*. 2013;22:5121–35.
- Tsurusaki Y, Koshimizu E, Ohashi H, Phadke S, Kou I, Shiina M, et al. De novo SOX11 mutations cause Coffin-Siris syndrome. *Nat Commun*. 2014;5:4011.
- Zweier C, Kraus C, Brueton L, Cole T, Degenhardt F, Engels H, et al. A new face of Borjeson-Forssman-Lehmann syndrome? De novo mutations in PHF6 in seven females with a distinct phenotype. *J Med Genet*. 2013;50:838–47.
- Bramswig NC, Caluseriu O, Ludecke HJ, Bolduc FV, Noel NC, Wieland T, et al. Heterozygosity for ARID2 loss-of-function mutations in individuals with a Coffin-Siris syndrome-like phenotype. *Hum Genet*. 2017;136:297–305.
- Vasileiou G, Vergarajauregui S, Ende S, Popp B, Buttner C, Ekici AB, et al. Mutations in the BAF-complex subunit DPF2 are associated with Coffin-Siris syndrome. *Am J Hum Genet*. 2018;102:468–79.
- The Deciphering Developmental Disorders S, Fitzgerald TW, Gerety SS, Jones WD, van Kogelenberg M, King DA, et al. Large-scale discovery of novel genetic causes of developmental disorders. *Nature*. 2014;519:223.
- Cherot E, Keren B, Dubourg C, Carre W, Fradin M, Lavillaureix A, et al. Using medical exome sequencing to identify the causes of neurodevelopmental disorders: experience of two clinical units and 216 patients. *Clin Genet*. 2018;93:567–76.
- Okamoto N, Ehara E, Tsurusaki Y, Miyake N, Matsumoto N. Coffin-Siris syndrome and cardiac anomaly with a novel SOX11 mutation. *Congenit Anom*. 2018;58:105–07.
- Jahani-Asl A, Cheng C, Zhang C, Bonni A. Pathogenesis of Borjeson-Forssman-Lehmann syndrome: Insights from PHF6 function. *Neurobiol Dis*. 2016;96:227–35.
- Mani U, Sankareswaran AS, Goutham RNA, Mohan SS. SWI/SNF infobase—an exclusive information portal for SWI/SNF remodeling complex subunits. *PLoS One*. 2017;12:e0184445.
- Sokpor G, Xie Y, Rosenbusch J, Tuoc T. Chromatin remodeling BAF (SWI/SNF) complexes in neural development and disorders. *Front Mol Neurosci*. 2017;10:243.
- Hota SK, Bruneau BG. ATP-dependent chromatin remodeling during mammalian development. *Development*. 2016;143:2882–97.
- Bevilacqua A, Willis MS, Bultman SJ. SWI/SNF chromatin-remodeling complexes in cardiovascular development and disease. *Cardiovascular Pathol*. 2014;23:85–91.
- Bogershausen N, Wollnik B. Mutational landscapes and phenotypic spectrum of SWI/SNF-related intellectual disability disorders. *Front Mol Neurosci*. 2018;11:252.
- Tsurusaki Y, Okamoto N, Ohashi H, Mizuno S, Matsumoto N, Makita Y, et al. Coffin-Siris syndrome is a SWI/SNF complex disorder. *Clin Genet*. 2014;85:548–54.
- Schrier SA, Bodurtha JN, Burton B, Chudley AE, Chiong MA, D'Avanzo MG, et al. The Coffin-Siris syndrome: a proposed diagnostic approach and assessment of 15 overlapping cases. *Am J Med Genet Part A*. 2012;158A:1865–76.
- Vergano SS, Deardorff MA. Clinical features, diagnostic criteria, and management of Coffin-Siris syndrome. *Am J Med Genet Part C Semin Med Genet*. 2014;166C:252–6.
- Campeau PM, Hennekam RC. DOORS syndrome: phenotype, genotype and comparison with Coffin-Siris syndrome. *Am J Med Genet Part C Semin Med Genet*. 2014;166C:327–32.
- Van Houdt JK, Nowakowska BA, Sousa SB, van Schaik BD, Seuntjens E, Avonce N, et al. Heterozygous missense mutations in

- SMARCA2 cause Nicolaides–Baraitser syndrome. *Nat Genet.* 2012;44:445–9.
23. Sekiguchi F, Nasiri J, Sedghi M, Salehi M, Hosseinzadeh M, Okamoto N, et al. A novel homozygous DPH1 mutation causes intellectual disability and unique craniofacial features. *J Hum Genet.* 2018;63:487–91.
 24. Aoi H, Lei M, Mizuguchi T, Nishioka N, Goto T, Miyama S, et al. Nonsense variants in STAG2 result in distinct sex-dependent phenotypes. *J Hum Genet.* 2019;64:487–92.
 25. Nord AS, Lee M, King MC, Walsh T. Accurate and exact CNV identification from targeted high-throughput sequence data. *BMC Genom.* 2011;12:184.
 26. Fromer M, Moran JL, Chambert K, Banks E, Bergen SE, Ruderfer DM, et al. Discovery and statistical genotyping of copy-number variation from whole-exome sequencing depth. *Am J Hum Genet.* 2012;91:597–607.
 27. Al-Shamsi A, Hertecant JL, Souid AK, Al-Jasmi FA. Whole exome sequencing diagnosis of inborn errors of metabolism and other disorders in United Arab Emirates. *Orphanet J Rare Dis.* 2016;11:94.
 28. Tsuchida N, Nakashima M, Kato M, Heyman E, Inui T, Haginoya K, et al. Detection of copy number variations in epilepsy using exome data. *Clin Genet.* 2018;93:577–87.
 29. Bogershausen N, Gatinois V, Riehrer V, Kayserili H, Becker J, Thoenes M, et al. Mutation update for kabuki syndrome genes KMT2D and KDM6A and further delineation of X-linked kabuki syndrome subtype 2. *Hum Mutat.* 2016;37:847–64.
 30. Miyake N, Abdel-Salam G, Yamagata T, Eid MM, Osaka H, Okamoto N, et al. Clinical features of SMARCA2 duplication overlap with Coffin–Siris syndrome. *Am J Med Genet Part A.* 2016;170:2662–70.
 31. Zarate YA, Bhoj E, Kaylor J, Li D, Tsurusaki Y, Miyake N, et al. SMARCE1, a rare cause of Coffin–Siris syndrome: clinical description of three additional cases. *Am J Med Genet Part A.* 2016;170:1967–73.
 32. Yu Y, Yao R, Wang L, Fan Y, Huang X, Hirschhorn J, et al. De novo mutations in ARID1B associated with both syndromic and non-syndromic short stature. *BMC Genom.* 2015;16:701.
 33. Mignot C, Moutard ML, Rastetter A, Boutaud L, Heide S, Billette T, et al. ARID1B mutations are the major genetic cause of corpus callosum anomalies in patients with intellectual disability. *Brain.* 2016;139:e64.
 34. Farwell KD, Shahmirzadi L, El-Khechen D, Powis Z, Chao EC, Tippin Davis B, et al. Enhanced utility of family-centered diagnostic exome sequencing with inheritance model-based analysis: results from 500 unselected families with undiagnosed genetic conditions. *Genet Med.* 2014;17:578.
 35. Santen GW, Aten E, Vulto-van Silfhout AT, Pottinger C, van Bon BW, van Minderhout IJ, et al. Coffin–Siris syndrome and the BAF complex: genotype–phenotype study in 63 patients. *Hum Mutat.* 2013;34:1519–28.
 36. Lower KM, Turner G, Kerr BA, Mathews KD, Shaw MA, Gedeon AK, et al. Mutations in PHF6 are associated with Borjeson–Forssman–Lehmann syndrome. *Nat Genet.* 2002;32:661–5.
 37. Tzschach A, Grasshoff U, Beck-Woedl S, Dufke C, Bauer C, Kehrer M, et al. Next-generation sequencing in X-linked intellectual disability. *Eur J Hum Genet.* 2015;23:1513–8.
 38. Mangelsdorf M, Chevrier E, Mustonen A, Picketts DJ. Borjeson–Forssman–Lehmann syndrome due to a novel plant homeodomain zinc finger mutation in the PHF6 gene. *J child Neurol.* 2009;24:610–4.
 39. Sen P, Luo J, Hada A, Hailu SG, Dechassa ML, Persinger J, et al. Loss of Snf5 induces formation of an aberrant SWI/SNF complex. *Cell Rep.* 2017;18:2135–47.
 40. Holsten T, Bens S, Oyen F, Nemes K, Hasselblatt M, Kordes U, et al. Germline variants in SMARCB1 and other members of the BAF chromatin-remodeling complex across human disease entities: a meta-analysis. *Eur J Hum Genet.* 2018;26:1083–93.
 41. Shibata M, Kanda M, Tanaka H, Umeda S, Miwa T, Shimizu D, et al. Overexpression of Derlin 3 is associated with malignant phenotype of breast cancer cells. *Oncol Rep.* 2017;38:1760–66.
 42. Prochasson P, Neely KE, Hassan AH, Li B, Workman JL. Targeting activity is required for SWI/SNF function in vivo and is accomplished through two partially redundant activator–interaction domains. *Mol Cell.* 2003;12:983–90.
 43. Ferreira ME, Prochasson P, Berndt KD, Workman JL, Wright AP. Activator-binding domains of the SWI/SNF chromatin remodeling complex characterized in vitro are required for its recruitment to promoters in vivo. *FEBS J.* 2009;276:2557–65.
 44. Ulirsch JC, Verboon JM, Kazerounian S, Guo MH, Yuan D, Ludwig LS, et al. The genetic landscape of Diamond–Blackfan anemia. *Am J Hum Genet.* 2018;103:930–47.
 45. Sanchis-Juan A, Stephens J, French CE, Gleadall N, Megy K, Penkett C, et al. Complex structural variants in Mendelian disorders: identification and breakpoint resolution using short- and long-read genome sequencing. *Genome Med.* 2018;10:95.
 46. Miao H, Zhou J, Yang Q, Liang F, Wang D, Ma N, et al. Long-read sequencing identified a causal structural variant in an exome-negative case and enabled preimplantation genetic diagnosis. *Hereditas.* 2018;155:32.

Affiliations

Futoshi Sekiguchi¹ · Yoshinori Tsurusaki^{1,2} · Nobuhiko Okamoto³ · Keng Wee Teik⁴ · Seiji Mizuno⁵ · Hiroshi Suzumura⁶ · Bertrand Isidor⁷ · Winnie Peitee Ong⁴ · Muzhirah Haniffa⁴ · Susan M. White^{8,9} · Mari Matsuo¹⁰ · Kayoko Saito¹⁰ · Shubha Phadke¹¹ · Tomoki Kosho¹² · Patrick Yap^{13,14} · Manisha Goyal¹⁵ · Lorne A. Clarke¹⁶ · Rani Sachdev¹⁷ · George McGillivray⁸ · Richard J. Leventer¹⁸ · Chirag Patel¹⁹ · Takanori Yamagata²⁰ · Hitoshi Osaka²⁰ · Yoshiya Hisaeda²¹ · Hirofumi Ohashi²² · Kenji Shimizu²² · Keisuke Nagasaki²³ · Junpei Hamada²⁴ · Sumito Dateki²⁵ · Takashi Sato²⁶ · Yasutsugu Chinen²⁷ · Tomonari Awaya^{28,29} · Takeo Kato²⁹ · Kougoro Iwanaga²⁹ · Masahiko Kawai²⁹ · Takashi Matsuoka³⁰ · Yoshikazu Shimoji³⁰ · Tiong Yang Tan^{8,9} · Seema Kapoor³¹ · Nerine Gregersen¹³ · Massimiliano Rossi³² · Mathieu Marie-Laure³² · Lesley McGregor³³ · Kimihiko Oishi³⁴ · Lakshmi Mehta³⁴ · Greta Gillies³⁵ · Paul J. Lockhart³⁵ · Kate Pope³⁵ · Anju Shukla³⁶ · Katta Mohan Girisha³⁶ · Ghada M. H. Abdel-Salam³⁷ · David Mowat³⁸ · David Coman³⁹ · Ok Hwa Kim⁴⁰ · Marie-Pierre Cordier⁴¹ · Kate Gibson⁴² · Jeff Milunsky⁴³ · Jan Liebelt⁴⁴ · Helen Cox⁴⁵ · Salima El Chehadeh⁴⁶ · Annick Toutain⁴⁷ · Ken Saida¹ · Hiromi Aoi^{1,48} · Gaku Minase¹ · Naomi Tsuchida¹ · Kazuhiro Iwama¹ · Yuri Uchiyama^{1,49,50} · Toshifumi Suzuki^{1,48} · Kohei Hamanaka¹ · Yoshiteru Azuma¹ · Atsushi Fujita¹ · Eri Imagawa^{1,34} · Eriko Koshimizu¹ · Atsushi Takata¹ · Satomi Mitsuhashi¹ · Satoko Miyatake^{1,50} · Takeshi Mizuguchi¹ · Noriko Miyake¹ · Naomichi Matsumoto¹

¹ Department of Human Genetics, Graduate school of medicine, Yokohama City University, Yokohama, Japan

² Faculty of Nutritional Science, Sagami Women's University, Sagamihara, Kanagawa, Japan

³ Department of Medical Genetics, Osaka Women's and Children's Hospital, Osaka, Japan

⁴ Department of Genetics, Hospital Kuala Lumpur, Kuala Lumpur, Malaysia

⁵ Department of Clinical Genetics, Central Hospital, Aichi Developmental Disability Center, Kasugai, Japan

⁶ Department of Pediatrics, Dokkyo Medical University, Tochigi, Japan

⁷ CHU Nantes, Service de Genetique Medicale, Nantes, France

⁸ Victorian Clinical Genetics Services, Murdoch Children's Research Institute, Melbourne, Australia

⁹ Department of Paediatrics, University of Melbourne, Melbourne, Australia

¹⁰ Institute of Medical Genetics, Tokyo Women's Medical University, Tokyo, Japan

¹¹ Department of Medical Genetics, Sanjay Gandhi Postgraduate Institute of Medical Sciences, Lucknow, India

¹² Department of Medical Genetics, Shinshu University School of Medicine, Matsumoto, Japan

¹³ Genetic Health Service New Zealand, Auckland, New Zealand

¹⁴ Faculty of Medical and Health Sciences, University of Auckland, Auckland, New Zealand

¹⁵ Rare Disease Clinic, J K Lone Hospital, SMS Medical College, Jaipur, Rajasthan, India

¹⁶ British Columbia Children's Hospital Research Institute, University of British Columbia, Vancouver, BC, Canada

¹⁷ Centre for Clinical Genetics, Sydney Children's Hospital,

Randwick, NSW, Australia

¹⁸ Royal Children's Hospital Department of Neurology, Murdoch Children's Research Institute and University of Melbourne Department of Pediatrics, Parkville 3052, Australia

¹⁹ Genetic Health Queensland, Royal Brisbane and Women's Hospital, Brisbane, QLD, Australia

²⁰ Department of Pediatrics, Jichi Medical University, Tochigi, Japan

²¹ Department of Neonatology, Japanese Red Cross Medical Center, Tokyo, Japan

²² Division of Medical Genetics, Saitama Children's Medical Center, Saitama, Japan

²³ Department of Homeostatic Regulation and Development, Niigata University Graduate School of Medical and Dental Sciences, Niigata, Japan

²⁴ Department of Pediatrics, Ehime University Graduate School of Medicine, Ehime, Japan

²⁵ Department of Pediatrics, Nagasaki University Graduate School of Biomedical Sciences, Nagasaki, Japan

²⁶ Asahikawa-Kosei General Hospital, Hokkaido, Japan

²⁷ Department of Child Health and Welfare, Graduate School of Medicine, University of the Ryukyus, Nishihara, Japan

²⁸ Department of Anatomy and Developmental Biology, Graduate School of Medicine, Kyoto University, Kyoto, Japan

²⁹ Department of Pediatrics, Graduate School of Medicine, Kyoto University, Kyoto, Japan

³⁰ Department of General Pediatrics, Okinawa Prefectural Nanbu Medical Center and Children's Medical Center, Okinawa, Japan

³¹ Division of Genetics, Department of Pediatrics, Maulana Azad Medical College, New Delhi, India

³² Hospices Civils de Lyon, Service de Génétique, Centre de Référence Anomalies du Développement, and INSERM U1028, CNRS UMR5292, CRNL, GENDEV Team, UCBL1 Bron, France

- ³³ South Australian Clinical Genetics Service, SA Pathology, Women's and Children's Hospital, Adelaide, Australia
- ³⁴ Department of Genetics and Genomic Sciences, Icahn School of Medicine at Mount Sinai, New York, NY, USA
- ³⁵ Bruce Lefroy Centre for Genetic Health Research, Murdoch Children's Research Institute, Victoria, Australia
- ³⁶ Department of Medical Genetics, Kasturba Medical College, Manipal, Manipal Academy of Higher Education, Manipal, India
- ³⁷ Department of Clinical Genetics, Human Genetics and Genome Research Division, National Research Centre, Cairo, Egypt
- ³⁸ Department of Medical Genetics, Sydney Children's Hospital, Sydney, NSW, Australia
- ³⁹ Department of Paediatrics, The Wesley Hospital, Brisbane, QLD, Australia
- ⁴⁰ Department of Radiology, Ajou University Hospital, Suwon, Korea
- ⁴¹ Service de Genetique, Hospices Civils de Lyon, Bron, France
- ⁴² Genetic Health Service New Zealand, Christchurch Hospital, Christchurch, New Zealand
- ⁴³ Center for Human Genetics Inc, Cambridge, MA, USA
- ⁴⁴ South Australian Clinical Genetics Services, Women's and Children's Hospital, North Adelaide, Australia
- ⁴⁵ West Midlands Regional Genetics Service, Birmingham Women's NHS Foundation Trust, Birmingham Women's Hospital, Edgbaston, Birmingham B15 2TG, UK
- ⁴⁶ Service de Genetique Medicale, Hopital de Haute-pierre, Strasbourg, France
- ⁴⁷ Service de Genetique, CHRU de Tours, Tours, France
- ⁴⁸ Department of Obstetrics and Gynecology, Juntendo University Faculty of Medicine, Tokyo, Japan
- ⁴⁹ Department of Oncology, Yokohama City University Graduate School of Medicine, Yokohama, Japan
- ⁵⁰ Clinical Genetics Department, Yokohama City University Hospital, Yokohama, Kanagawa, Japan